Received: 18 December 2019 | Revised: 10 June 2020 | Accepted: 15 June 2020

DOI: 10.1002/nbm.4367

RESEARCH ARTICLE

NMR IN BIOMEDICINE WILEY

Protein conformational changes affect the sodium triple-quantum MR signal

Dennis Kleimaier[1] | Victor Schepkin[2] | Ruomin Hu[1] | Lothar R. Schad[1]

[1]Computer Assisted Clinical Medicine, Heidelberg University, Mannheim, Germany

[2]National High Magnetic Field Laboratory, Florida State University, Tallahassee, USA

Correspondence
Dennis Kleimaier, Computer Assisted Clinical Medicine, Theodor-Kutzer-Ufer 1-3, 68167, Mannheim, Germany.
Email: dennis.kleimaier@medma.uni-heidelberg.de

Funding information
National Science Foundation, Grant/Award Number: NSF/DMR-16644779

The aim of this study was to investigate possible sodium triple-quantum (TQ) signal dependence on pH variation and protein unfolding which may happen *in vivo*. The model system, composed of bovine serum albumin (BSA), was investigated over a wide pH range of 0.70 to 13.05 and during urea-induced unfolding. In both experimental series, the sodium and BSA concentration were kept constant so that TQ signal changes solely arose from an environmental change. The experiments were performed using unique potential to detect weak TQ signals by implementing a TQ time proportional phase increment pulse sequence. At a pH of 0.70, in which case the effect of the negatively charged groups was minimized, the minimum TQ percentage relative to single-quantum of 1.34% ± 0.05% was found. An increase of the pH up to 13.05 resulted in an increase of the sodium TQ signal by 225%. Urea-induced unfolding of BSA, without changes in pH, led to a smaller increase in the sodium TQ signal of up to 40%. The state of BSA unfolding was verified by fluorescence microscopy. Results of both experiments were well fitted by sigmoid functions. Both TQ signal increases were in agreement with an increase of the availability of negatively charged groups. The results point to vital contributions of the biochemical environment to the TQ MR signals. The sodium TQ signal *in vivo* could be a valuable biomarker of cell viability, and therefore possible effects of pH and protein unfolding need to be considered for a proper interpretation of changes in sodium TQ signals.

KEYWORDS
bovine serum albumin, electric quadrupole interaction, protein folding, sodium NMR, sodium triple-quantum signal, triple-quantum time proportional phase increment

Abbreviations used: BSA, bovine serum albumin; DQ, double-quantum; FID, free induction decay; FWHM, full width at half maximum; PCC, Pearson correlation coefficient; RF, radiofrequency; SQ, single-quantum; TQ, triple-quantum; TQTPPI, triple-quantum time proportional phase increment.

1 | INTRODUCTION

The biological and physical properties of the sodium nucleus are attractive for a variety of biomedical MR applications.[1,2] The sodium potassium pump maintains a large sodium concentration difference between the intra- and extracellular space.[2] Maintaining this difference in sodium concentration is a highly energy-consuming process. Therefore, sodium MR signals may directly reflect disruption in energy metabolism on a cellular level and, therefore, may aid in the noninvasive detection and investigation of vital *in vivo* processes.

The sodium nucleus has a nuclear spin of 3/2. This allows the positively charged sodium ions (Na^+) to interact with surrounding electric field gradients created by electro-negative groups within macromolecules during electrostatic attraction or binding. These charged groups include carboxyl, hydroxyl and phosphate groups of proteins, nucleic acids and carbohydrates.[3] In this case, binding refers to electric quadrupole interactions of sodium ions with electro-negative groups during a time range of several milliseconds. Interactions in this time range create observable sodium triple-quantum (TQ) signals. It was shown that the sodium TQ signal may have a higher intracellular weighting than the sodium single-quantum (SQ) signal.[4–11] Thus, the TQ signal can potentially be a valuable biomarker of cell viability.[4,6,7,12–16] Both the sodium TQ signal and the sodium SQ signal can be valuable parameters for cell viability.[17–22] Yet, in the case of the sodium SQ signal, the differentiation between increased intracellular sodium content and increased extracellular space cannot be accomplished.[23] Therefore, combined approaches[24–26] which simultaneously measure the sodium SQ and TQ signal may further enhance the value of sodium MRI. However, the interpretation of the biological origin of the TQ signal should be performed very carefully as it may be hindered by many biological and physical environmental factors. For instance, TQ signals were shown to depend on the concentrations of sodium[4,7] and protein.[7,11] Furthermore, changes in the extracellular sodium TQ signal,[4,27] altered transversal relaxation times,[28,29] and competitive binding with ions such as potassium[3] or lithium[30] should be taken into consideration.

Another important factor that may influence the sodium TQ signal is the availability of negatively charged groups of proteins induced by pH or protein conformational changes (Figure 1). Possible causes of a pH change *in vivo* are cancer or stop-flow ischemia, while protein conformational changes are associated with cancer or neurodegenerative diseases. In cancerous tissue, the intracellular pH and the extracellular pH can change from 7.05-7.2 to 7.3-7.6 and from 7.4 to 6.8-7.0, respectively.[31] During brain ischemia, both the extra- and intracellular pH could drop to 6.2-6.9 depending on the duration of ischemia.[32–34]

At higher pH values, the availability of negatively charged groups of macromolecules increases, while at lower pH values it decreases (Figure 1A). In addition, a pair of oppositely charged groups within close-range can interact noncovalently via electrostatic interaction, forming an ion pair.[35] As the availability of electro-negative and electro-positive groups varies with pH, the number of such ion pairs also differs. The alteration of negatively charged groups by pH results in a changed affinity of proteins for cations.[36–38] In accordance with these studies, Hutchison et al[39] observed a change in a sodium double-quantum (DQ) signal from bovine serum albumin (BSA) in solution with a pH range of 5 to 8. It is expected that not only DQ signal, but also a sodium TQ signal originating during binding interactions between proteins and sodium ions, will depend on pH.

The 3D structural integrity of proteins is a fundamental part of their biological function. Unfolding of proteins results in the disruption of the tertiary and secondary protein structure and in the exposure of the protein backbone to the aqueous phase.[40–42] This can increase the availability of negatively charged groups, as ion pairs are disrupted and amino acid residues buried in the hydrophobic protein core become exposed to the

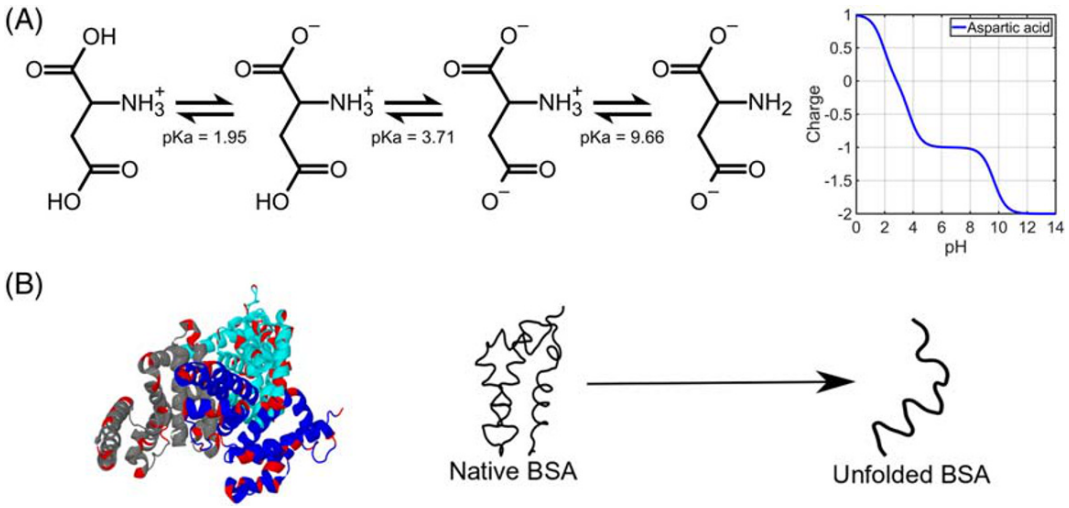

FIGURE 1 (A) The relation between the electric charge of the carboxyl groups and pH is shown for the amino acid aspartic acid. The charge of each carboxyl group depends on the acidity constant pKa as well as the solution pH. (B) The unfolding of BSA leads to a random coil configuration. On the left, the native BSA crystal structure is visualized (PDB-File: 4F5S). BSA domain I (gray), II (cyan), III (blue), and the negatively charged amino acid residues (red)

aqueous phase[43] (Figure 1B). This environmental change can influence the electric-quadrupole interactions of sodium ions with negatively charged groups, thereby affecting sodium relaxation times and, thus, sodium TQ signal. Therefore, we hypothesize that the TQ signal may depend on the protein folding state.

The goal of the current study is an evaluation of effects on the sodium TQ signal caused by changes in pH as well as the protein folding state. The concurrent changes in sodium relaxation times were also evaluated.

In this study, the TQ time proportional phase increment (TQTPPI) pulse sequence[3,12,13] was selected for sensitive detection of sodium TQ signals. The sodium TQ signal was separated by frequency from other MR signals comprising SQ and DQ signals. The pulse sequence allows the equal optimal detection of sodium TQ signals with different ion binding interaction strengths. The DQ signal was suppressed and SQ signal served as a reference quantification parameter.[44] The TQ/SQ signal ratio has been shown to be capable of reflecting the level of sodium interactions with macromolecules.[3,12,13]

The experiments in this study were conducted using BSA, a protein that has been shown to create a strong TQ signal despite a weak affinity for sodium ions.[36,45–47] BSA was selected to be a suitable model system, as BSA has been widely studied, is available in high purity, and has a known protein structure with a relatively large amino acid chain length of 583. The number of negatively charged amino acids is 100 (59 glutamic acid, 40 aspartic acid and one carboxyl-terminus). Furthermore, both the distribution of correlation times and the root mean square of the electric quadrupole interactions of BSA are very similar to the yeast protoplasm.[46] The pH dependence was investigated by measuring the sodium TQ signal of 10% *w/v* BSA over a wide pH range of 0.70 to 13.05, while the sodium and BSA concentration were kept constant. Extreme pH values were chosen to obtain an estimate of the minimum and maximum TQ signal of 10% *w/v* BSA. The influence of the protein conformation on the sodium TQ signal was studied under constant pH and by using urea-induced unfolding of BSA. The use of urea does not induce formation of immobile solid-like structures.[48] The state of BSA unfolding was additionally monitored by fluorescence signals from two tryptophan residues.[49]

2 | MATERIALS AND METHODS

2.1 | Model solutions and variation of the pH values

All chemical substances used to produce the phantoms were purchased from Carl Roth GmbH (Karlsruhe, Germany). In the first step, saline solutions were made by adding 154 mM NaCl to distilled water. Such saline solutions are pH-neutral. To increase or decrease the pH of such solutions, a portion of the saline solution was replaced by an alkaline solution containing 154 mM NaOH or by an acidic solution containing 100 mM HCl with 154 mM NaCl, respectively. The final pH of the solution was verified with a VOLTCRAFT PH-100 ATC device (Conrad Electronic SE, Wernberg, Germany) after MRS measurements.

The 24 phantoms (diameter = 16mm and length = 40mm) containing 8ml solution with 154 mM Na^+ and 10% *w/v* BSA were prepared with nonequidistantly distributed pH values over the range of 0.70 to 13.05. The extremely low pH values should minimize the availability of all negatively charged groups, while a pH 13.05 should maximize the availability of all negatively charged groups for sodium binding.[50]

2.2 | Urea-induced unfolding of BSA

For the following control and urea-induced unfolding of BSA experiments, 10 ml phantoms (diameter = 16 mm and length = 50 mm) with 154 mM NaCl were prepared.

2.2.1 | Control experiments

The control measurements served to determine if the presence of urea itself might create a sodium TQ signal. For this purpose, phantoms with a urea concentration of 0, 5.5 and 8 M were used. All three phantoms contained no BSA.

2.2.2 | BSA unfolding experiments

In these experiments, the urea concentrations had the values of 0, 1, 2, 3, 4, 5, 5.5, 6, 7 and 8 M. All 10 phantoms contained 5% *w/v* BSA. The pH values were 7.02, 7.03, 7.05, 7.05, 7.03, 7.00, 6.98, 6.99, 7.04 and 7.05 in phantoms with a urea concentration of 0, 1, 2, 3, 4, 5, 5.5, 6, 7 and 8 M, respectively. The low content of BSA was chosen to prevent gelation of BSA occurring at high urea concentrations.[51] No gelation of BSA was observed during an observation period of 3 months following our experiments, during which the phantoms were stored at room temperature.

2.3 | Fluorescence measurements

Fluorescence measurements were used as a gold standard to monitor the protein folding state. A second set of phantoms was produced for such measurements, identical to the ones used in MR experiments. Fluorescence was monitored by a Tecan Infinite 200 PRO plate reader (Tecan Group, Männedorf, Switzerland) using three 200 μl volumes per phantom. The two tryptophan residues of BSA were excited at λ = 295 nm with a subsequent detection of response between λ = 320 nm and λ = 400 nm with a resolution of $\Delta\lambda$ = 2 nm. The detected fluorescence spectra were integrated, and the relative changes were plotted as a function of urea concentration to obtain a denaturation curve.

2.4 | MRS measurements

MR sodium data were acquired using a 9.4 T preclinical scanner (Biospec 94/20, Bruker, Ettlingen, Germany) equipped with a linear polarized $^{1}H/^{23}Na$ Bruker volume coil. The volume coil with an inner diameter of 72 mm had a length of 110 and 100 mm for ^{1}H and ^{23}Na, respectively.

The non-localized TQTPPI pulse sequence consisted primarily of three 90° radiofrequency (RF) pulses. One additional 180° refocusing RF pulse was set in the middle between the first two 90° RF pulses, to compensate for B_0 inhomogeneity (Figure 2A). The time interval between the first and the second 90° RF pulses, called the evolution time (τ_{evo}), was incremented in the pulse sequence. The interval between the second and third 90° RF pulses, called the mixing time (τ_{mix}), was set for its minimum possible value and remained unchanged. In our case, τ_{mix} was in the range of 130-135 μs. The starting phase α = 90° was incremented in 45° steps, resulting in a cycle of eight phase steps to cover a full rotation of 360°. To suppress sodium DQ signals, phase β was alternated between ±90° while keeping τ_{evo} unchanged. An additional eight phase steps were added, extending the total number of phase steps in one phase cycle to 16. The signals of these two subsequent phase steps were added to suppress the DQ signal. Figure S1 and Figure 2 show the successful suppression of the DQ signal. Next, the evolution time was incremented by $\Delta\tau_{evo}$ alongside an increment of α by 45° after every second phase step. The total number of increments (ns) is given by ns = 8*n_{PC}, where n_{PC} is the number of phase cycles.

The first free induction decay (FID) was Fourier-transformed and phase-corrected by an automatic phasing in frequency domain. Then the found phase correction was applied to all other FIDs. Subsequently, all spectra were stacked along the evolution time axis. The amplitudes of sodium spectral peak constituted the amplitudes of the TQTPPI FID in a second dimension. A Fourier transform of this TQTPPI FID yielded the TQTPPI spectrum showing an SQ and a TQ peak at distinct frequencies (Figure 2B).

The length of the 90° RF pulse and therefore τ_{mix} was 130-135 μs. The original FIDs had 2048 complex points and a sampling rate of 50 μs per complex point. The number of phase cycles, n_{PC} = 50-100, was selected to sample the entire TQTPPI FID decay in a second dimension. The evolution time increment ($\Delta\tau_{evo}$) was 200 μs and the range of the evolution time was τ_{evo} = 0.4-160.4 ms. The T_1 value of each phantom was measured in advance, enabling a repetition time of $T_R > 5\ T_1$ (or T_R = 125-300 ms) to be set for the TQTPPI measurements. The total scan duration for one TQTPPI measurement was in the range of 2.2-10.1 minutes. Each phantom measurement was repeated 4-7 times with three averages.

To fit the TQTPPI FID, a Matlab (MathWorks, Natick, MA, USA) built-in trust region-based algorithm[52] was used. The TQTPPI FID fit function was[3]:

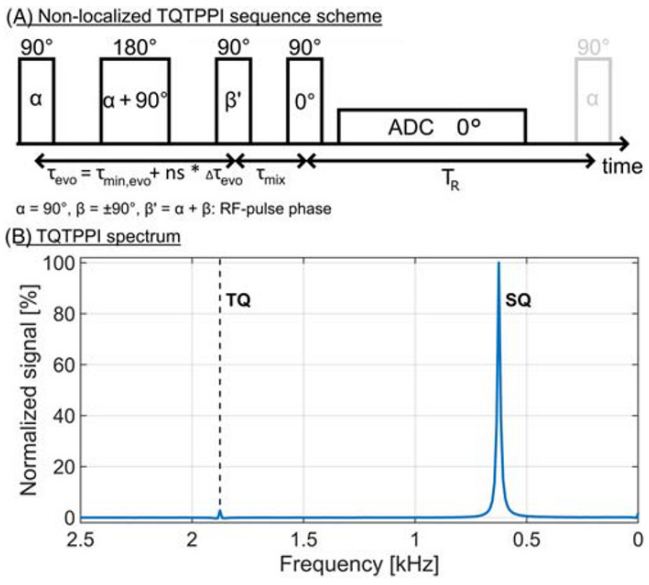

FIGURE 2 (A) The TQTPPI pulse sequence. In this pulse sequence, the RF phase α = 90° + ns * 45° and the evolution time $\tau_{evo} = \tau_{min,evo} + ns * \Delta\tau_{evo}$ are simultaneously incremented. For elimination of the DQ signal, the output signals for the RF phases β = ±90° are added for each new value of α and τ_{evo}. A 180° refocusing RF pulse during the evolution time compensates for B_0 inhomogeneities. (B) Sodium TQTPPI spectrum of 10% *w/v* BSA with pH 13.05 and $\Delta\tau_{evo}$ = 0.2 ms. The TQTPPI spectrum consists of sodium SQ and TQ signals at the distinct frequencies of 0.625 and 1.875 kHz, respectively. The sodium DQ signal, which should appear at the frequency of 1.25 kHz, was completely eliminated

$$S(t) = A_{SQS} \sin(\omega t + \varphi_1) \exp(-t/T_{2S}) + A_{SQF} \sin(\omega t + \varphi_1) \exp(-t/T_{2F}) + A_{TQ} \sin(3\omega t + \varphi_2) (\exp(-t/T_{2F}) - \exp(-t/T_{2S})) + DC \quad (1)$$

The parameters A_{SQS} and A_{SQF} are the amplitudes of the slow and the fast SQ relaxation component, respectively. Similarly, T_{2S} and T_{2F} are the respective slow and fast transversal relaxation times. A_{TQ} is the amplitude of the TQ signal. The frequency ω in the second dimension is defined by $\omega = 1/((360^\circ/\Delta\alpha)\ \Delta\tau_{evo})$, where $\Delta\alpha = 45^\circ$. Possible phase shifts are compensated by φ_1 and φ_2; DC is a base line shift. In the current study, we report the TQ amplitude as $(A_{TQ}/(A_{SQS} + A_{SQF}))$, that is, normalized to the total SQ amplitude A_{SQ}. Additionally, we report the fraction of the slow component (A_{SQS}/A_{SQ}), and both transverse relaxation times, T_{2S} and T_{2F}. Each TQTPPI measurement was fitted separately to determine the mean and the standard deviation of all fitting parameters.

2.5 | Quantification of protein conformational changes

The relative change of the sodium TQ signal and integrated fluorescence signal during urea-induced unfolding of BSA was calculated by using the measurements at c_{urea} = 0 M as a reference. Measurement data from investigation of pH and the protein folding state Y(x) were fitted by a sigmoid function, which is commonly used for investigation of pH[53] dependence and the protein folding state[48,49]:

$$Y(x) = A + (B - A)/(1 + \exp((V_{50} - x)\, C)) \quad (2)$$

For the pH experiment, *A* and *B* are the minimum and maximum values of the sodium TQ signal, respectively, and x represents the pH value. For the urea experiment, *A* and *B* are the minimum and maximum values, respectively, of the relative change of either the TQ or fluorescence signal. In this case, x is the urea concentration. V_{50} is the transition midpoint and C is the growth rate of the sigmoid function. For the fitting of the data from urea-induced unfolding of BSA, the minimum value a was set to zero.

2.6 | Statistical analysis

The signal-to-noise ratio (SNR) of the TQ signal was calculated via SNR = (peak height)/σ_{noise}, where σ_{noise} is the standard deviation of the data points in the TQTPPI spectrum containing only noise signal. SNR was used as a measure of the significance for the sodium TQ signal. For a TQ| SNR| < 3, the TQTPPI FID was fitted by mono-exponential decay, while the TQ signal fitting was omitted.[12] The Pearson correlation coefficient (PCC) was used for correlation analysis.

3 | RESULTS

3.1 | Variation of the pH value

The dependence of the sodium TQ signal on pH was investigated in phantoms with 10% *w/v* BSA and 154 mM Na^+ over the pH range of 0.70 to 13.05. The changes of the TQ signal, the amplitude of the slow relaxing component and both T_2 relaxation times as a result of the variation of pH are presented in Figure 3. In the pH region of 3.55 to 6.50, the A_{TQ}/A_{SQ} ratio was unchanged within the 95% confidence interval (CI) and the average A_{TQ}/A_{SQ} was 1.59% ± 0.12%. When pH was increased from 6.50 to 8.84, the A_{TQ}/A_{SQ} values increased almost linearly with pH. In the phantoms with a pH of 8.84 to 9.64, the A_{TQ}/A_{SQ} ratio reached a constant value of 5.16% ± 0.09%, which is a ∼225% increase relative to the average value of A_{TQ}/A_{SQ} in the pH region of 3.55 to 6.50. In addition to the increase in the TQ signal, both sodium T_2 relaxation times decreased with increasing pH, while T_{2F} decreased at a higher rate than T_{2S}. The T_1 values were close to the corresponding T_{2S} values for all phantoms (Figure S2a). It is important to note that in the pH range of 3.55 to 9.56, the amplitude ratios of A_{SQS}/A_{SQ} were unchanged at 41.2% ± 0.9% (Figure 3A).

The sodium TQ signal at the extremely low pH of 0.70 to 2.09 was constant within 95% CI and the average A_{TQ}/A_{SQ} ratio was 1.27% ± 0.07%. This was a reduction by 20% ± 7% compared with the average A_{TQ}/A_{SQ} ratio of 1.59% ± 0.12% at a pH of 3.55 to 6.50. At pH 13.05, the A_{TQ}/A_{SQ} ratio was 5.22% ± 0.13%, which was within 95% CI compared with the A_{TQ}/A_{SQ} ratio of 5.16% ± 0.09% for a pH of 8.84 to 9.64. Thus, the maximum TQ signal was already reached at a pH of 8.84. The ratio of the slow amplitudes (A_{SQS}/A_{SQ}) was 58.8% ± 0.9% and 45.6% ± 2.9% for pH values of 0.70 to 2.09 and 13.05, respectively. The fitting analysis of the TQ measurements during pH variation by a sigmoid function (Equation 2) yielded a transition midpoint at a pH of 7.60 ± 0.11 and a growth rate of 2.05 ± 0.40 1/pH (Table 1).

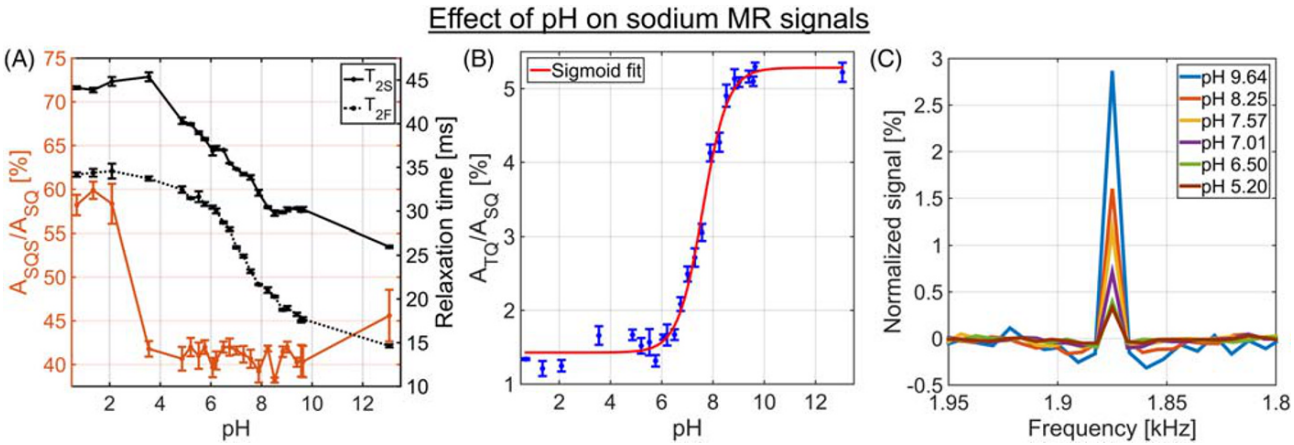

FIGURE 3 (A) Dependence of sodium T_2 relaxation times and the fraction of the slow component A_{SQS}/A_{SQ} on pH in the BSA phantom samples. At the high pH values, T_{2F} was decreasing much faster compared with T_{2S}. (B) Dependence of the sodium TQ signal on pH in the phantom samples. Up to pH 6.50, A_{TQ}/A_{SQ} remains relatively unchanged. Between pH 6.5 and 8.84, the A_{TQ}/A_{SQ} increased with pH, which correlates with the fact that at higher pH values the electrostatic attraction to the negatively charged groups is increasing. The results of the sigmoid fit are given in Table 1. (C) Zoomed sodium TQTPPI spectra for different pH values

TABLE 1 Sigmoid function fit of the results for sodium TQ MR signal and fluorescent response

Fit parameter	A_{TQ}/A_{SQ} vs pH	A_{TQ}/A_{SQ} vs c_{urea}	Fluorescence signal vs c_{urea}
A	1.43 ± 0.12%	0%	0%
B	5.28 ± 0.18%	43.22 ± 11.64%	46.04 ± 7.94%
V_{50}	7.60 ± 0.11 pH	5.73 ± 0.60 M	5.92 ± 0.35 M
C	2.05 ± 0.40 1/pH	1.48 ± 1.14 1/M	1.89 ± 1.06 1/M

Sigmoid function is presented by Equation 2. "A" is the minimum value, "B" is the maximum value, "V_{50}" is the transition midpoint of the sigmoid function and "C" is the growth rate.

3.2 | Urea-induced unfolding of BSA

In control experiments, no significant sodium TQ signal was found. The TQ SNR was −2.4, −0.1 and 1.0 (±0.1) for 0, 5.5 and 8 M urea, respectively. The result of the control TQTPPI experiment in the phantom containing 8 M urea without BSA is illustrated in Figure 4D. By contrast, a significant TQ SNR of at least 24.3 ± 0.1 was measured in phantoms containing BSA during the unfolding experiments. Thus, the presence of urea did not produce any background sodium TQ signal in our BSA unfolding experiments.

In the same control measurements, without BSA, sodium at the higher urea concentrations had lower T_2 relaxation times, 50.6, 34.7 and 25.2 (±0.1) ms for the samples with 0, 5.5 and 8 M urea, respectively. In the unfolding experiments, a similar reduction in all sodium relaxation times was observed, where the T_1 values were again close in value to T_{2S} (Figure 4A and Figure S2b).

In Figure 4B, the change in the sodium TQ signal in the unfolding experiments is presented. Up to a urea concentration of 4 M, the relative change in the TQ signal was almost zero, within 95% CI, relative to the 0 M urea sample. For higher urea concentrations, the sodium TQ signal increased and reached a constant value above 7 M urea. In addition to these changes in the sodium TQ signal, the fraction of the slow component A_{SQS}/A_{SQ} changed from 49.5% ± 4.2% (0 M urea) to 59.6% ± 4.6% for 1-2 M urea and reached a plateau of 52.1% ± 1.9% for 3-5.5 M urea (Figure 4A). For 6-8 M urea, the T_{2S} fraction was 42.2% ± 1.1%.

The above observed sodium TQ signal changes were compared with the results of an established method to detect protein unfolding using fluorescence measurements, where the signals from two intrinsic tryptophan residues of BSA were used.[49] The changes of the fluorescence spectra reflecting the protein denaturation are presented in Figure 4B,C. Using the reverted A_{TQ}/A_{SQ} y-axis, the results of the TQ experiments were overlaid with data from the fluorescence experiments (Figure 4B). Both experiments revealed a similar sigmoidal shape dependence during BSA unfolding. Correlation analysis showed a negative linear correlation of A_{TQ}/A_{SQ} with the fluorescence signal (PCC = −0.99, $P < .01$), which indicated a high correlation of the TQ signal with the protein structural alterations. A sigmoid fit of both denaturation curves also revealed a comparable transition midpoint at ∼ 5.7-5.9 M urea (Table 1). In both denaturation curves, a complete unfolding of BSA was reached above 7 M urea.

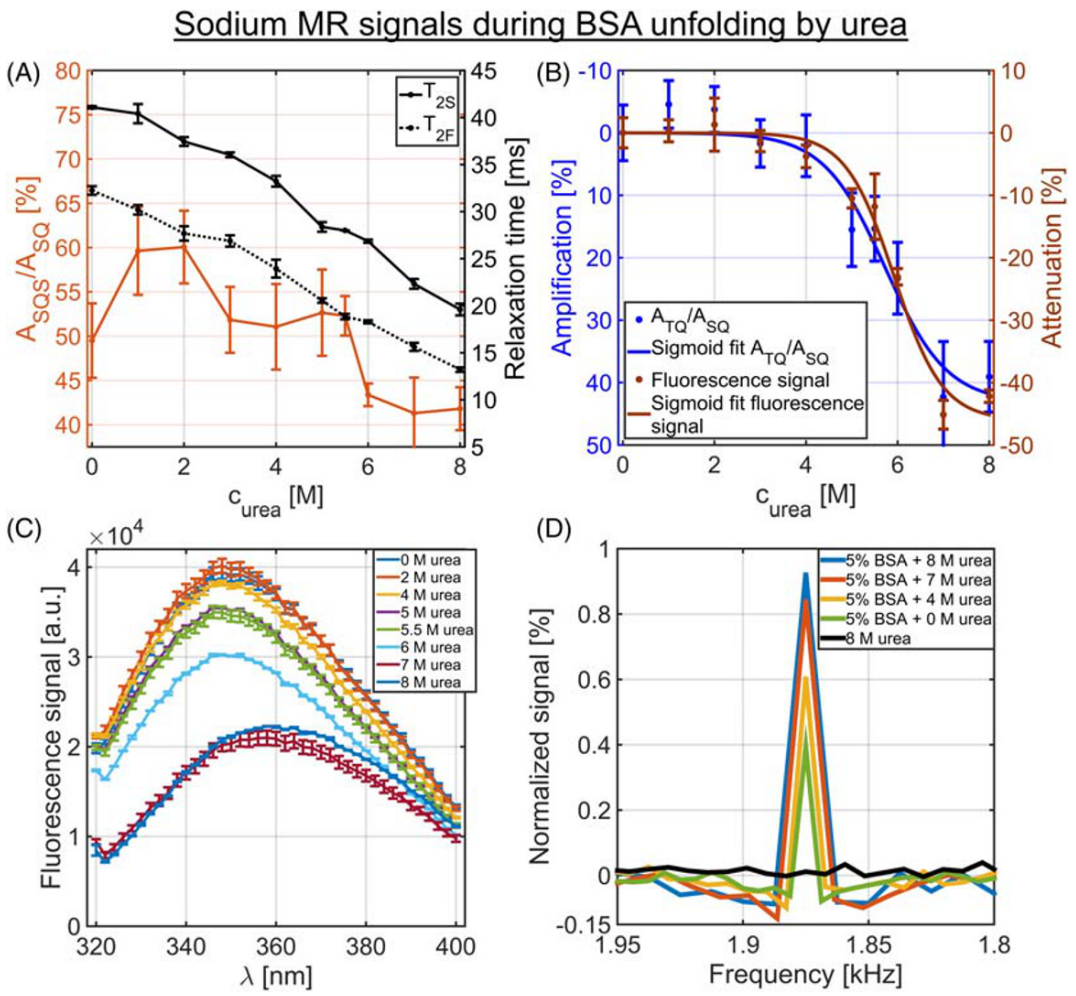

FIGURE 4 (A) Dependence of sodium T_2 relaxation times and the fraction of the slow component A_{SQS}/A_{SQ} on urea concentration in the BSA phantom samples during the unfolding experiments. The addition of urea caused a reduction in both sodium transverse relaxation times and in the percentage of slow relaxing component. (B) Comparison of the A_{TQ}/A_{SQ} ratio and the fluorescence signal at different urea concentrations in the phantom samples during the BSA unfolding experiments. The A_{TQ}/A_{SQ} y-axis was inverted for a better comparison of the shapes of the TQ signal with denaturation curve detected by fluorescence signal. For calculation of the relative changes in both curves, the measurement with 0 M urea was used as a 100% reference. Both denaturation curves show a similar sigmoidal shape (Table 1) and the correlation analysis revealed a negative linear correlation of the A_{TQ}/A_{SQ} ratio to the fluorescence signal (PCC = −0.99). (C) Fluorescence spectra of 5% *w/v* BSA at different urea concentrations. Protein unfolding reduces the fluorescence signal. (D) Zoomed TQTPPI spectra of 5% *w/v* BSA at different urea concentrations as well as for 8 M urea without BSA are shown. Urea alone, without BSA, even at the urea concentration of 8 M does not create any sodium TQ signal

4 | DISCUSSION

The sodium TQ signal is created when positively charged sodium ions interact with negatively charged groups of macromolecules (e.g. proteins). Such signals can be used to assess cell viability.[4,6,7,12–16] However, the effect of pH or protein conformation, which affects the availability of negatively charged groups, can contribute to the TQ signal and needs to be evaluated. In this study, we investigated the dependence of the sodium TQ signal on pH and the protein folding state of the well-known protein BSA, which can resemble the in vivo situation.[46] The pH dependence was evaluated for 10% *w/v* BSA over a wide pH range of 0.70 to 13.05. The influence of the protein folding state on the TQ signal was investigated by urea-induced BSA unfolding. These results provide insights giving a deeper understanding of the origin of the sodium TQ signal and its capability to serve as a potential biomarker.

In general, negatively charged groups within proteins are mainly found in the carboxyl-terminus and the amino acids, aspartic acid and glutamic acid. The observed increase in A_{TQ}/A_{SQ} by ∼225% for a pH range of 6.50 to 8.84 can be explained by a combination of the following two effects: (i) the protonation level of each carboxyl group depends on the dissociation constant pKa. At low pH, almost all carboxyl groups are protonated and therefore are almost neutrally charged. With increasing pH, the availability of negatively charged groups increases as more carboxyl

groups become deprotonated or more negatively charged; and (ii) oppositely charged groups of proteins within close range can interact via electrostatic interactions and form ion pairs. These ion pairs can contribute to the overall stability of the protein tertiary structure,[35] while their numbers and strength of interaction also depend on pH. For increasing pH, the increase in available negatively charged groups and the reduction of available positively charged groups decreases the number of ion pairs, which also increases the availability of the negatively charged groups.[42] Both effects lead to an increase in the availability of negatively charged groups and can contribute to the observed increase of A_{TQ}/A_{SQ} with increasing pH. However, which effect is more dominant has yet to be investigated. But the large increase in TQ signal during variation of pH underlines the importance of the availability of negatively charged groups for the creation of a TQ signal. Increasing pH also caused a reduction in transversal relaxation times, which was also demonstrated for human erythrocytes over a pH range of 5.2 to 8.5.[54] The reduction in relaxation times and increase of the TQ signal for increasing pH are in accordance with the observed higher affinity of proteins for cations with increasing pH.[36–38]

The extreme variation in pH can cause denaturation of BSA. According to Lin and Koenig,[55] the onset of acidic and alkaline denaturation of BSA is found around pH 5.0 and 9.5-10.0, respectively. For the pH range of 6.50 to 8.84, denaturation of BSA is not expected and therefore the increased TQ signal in this pH range was a consequence of the reasons mentioned above. However, denaturation of BSA could have influenced the estimation of the minimum and maximum TQ signals of 10% *w/v* BSA. For pH 0.70 to 2.09, an average TQ signal of A_{TQ}/A_{SQ} = 1.27% ± 0.07% was still found. In particular, at pH 0.70, the effect of negatively charged groups on TQ signal is minimized, because almost all of the negatively charged groups are protonated and therefore neutrally charged.[50] For these very low pH values, the slow relaxing fraction of sodium signal A_{SQS}/A_{SQ} changed to 58.8% ± 0.9% compared with 41.2% ± 0.9% for pH 3.55 to 9.56. The deviation of A_{SQS}/A_{SQ} from the theoretically expected value of 40% at low pH suggests that sodium ions were exposed to multiple environments with different bi-exponential or mono-exponential relaxation properties.[56] The fact that the TQ signal was unchanged in the pH range of 0.70 to 2.09 can be attributed to protein unfolding and aggregation of BSA. At these low pH values, amine groups are positively charged (Figure 1A) and, in combination with aggregation of BSA, could cause electric quadrupole interactions which are sufficient for the creation of a TQ signal. Further investigations of different proteins with a minimized influence of negatively charged groups using the sodium TQ signal are required to confirm this observation.

The observed pH dependence may affect the analysis of the sodium TQ signal in pathologies such as ischemic stroke[32–34] or tumor.[31,57] LaVerde et al[16] investigated the sodium TQ signal in focal brain ischemia of a nonhuman primate model. After 0.6 hours the TQ signal increased by 126% ± 70%, and after 3 hours by 175% ± 91%. It was concluded that these changes were only caused by an increased intracellular sodium concentration. However, both extra- and intracellular pH could drop to 6.2-6.9 during ischemia, depending on the duration of ischemia.[32–34] According to estimates from the current study, a decrease in pH from 7 to 6.5 could cause a A_{TQ}/A_{SQ} reduction of 33% ± 4%. Thus, the actual increase of the TQ signal due to changes in the intracellular sodium content might have been larger than the values reported by LaVerde et al,[16] as both the extra- and intracellular TQ signal could have been decreased by reduced pH. It is important to note that alterations in the TQ signal due to changes in the intracellular sodium content or pH cannot be separated. To exclude the effect of pH changes on the TQ signal, MRI-based methods to assess the pH can be used.[58–60]

Thus, in addition to biological and physical environmental factors, such as sodium and protein concentration, the TQ signal depends on the availability of negatively charged groups and therefore on the pH value. This should be considered in the interpretation of TQ signals from pathologies causing a pH change, for example, ischemic conditions.[9,11–13,61–64] This pH dependence, however, cannot be used to directly measure the pH value, as sodium interactions with macromolecules are needed for the TQ signal. Thus, without macromolecules, pH variation may lead to small changes in sodium relaxation times.

Going one step further, a possible correlation between the TQ signal and the protein folding state was investigated. Protein folding states include natively folded proteins, partially folded proteins, unfolded proteins and protein aggregates.[42] Only the native protein structure possesses a biological function.

In the control measurements of NaCl with urea, a strong reduction of the relaxation times was observed, which was not accompanied by the formation of a TQ signal. Schepkin et al[3] observed a similar effect in solutions of glycerol and saline in equal volumes. They measured an even more substantial reduction of the relaxation times and, similarly, did not detect any TQ signal due to the very short tumbling time of the glycerol molecule. The tumbling time of the urea molecule is also too short for the formation of a TQ signal and thus the presence of urea did not contribute to a measured increase of the TQ signal in our unfolding experiments.

The urea-induced unfolding of BSA resulted in an increase of the sodium TQ signal with a sigmoid function profile similar to fluorescence measurements. Both methods have similar curves as a function of urea concentration with a negative linear correlation (PCC = −0.99), indicating a correlation of the TQ signal with the changes in protein structure. The pH value was practically unchanged, and it was verified directly after each MRS measurement in each phantom to control a possible pH effect on the urea experiments.

Urea unfolds proteins, due to the preferential solvation of hydrophobic residues and the preferential binding of urea to the protein backbone.[40,41] Protein unfolding by urea disrupts the protein tertiary and secondary structure and exposes the protein backbone to the aqueous phase.[42] These effects lead to a random coil formation of the protein (Figure 1). The observed increase of the sodium TQ signal in the BSA unfolding experiment can be explained by a combination of two effects: (i) the loss of the tertiary structure disrupts ion pairs, which increases the availability of negatively charged groups compared with the native state. However, it has recently been suggested that in denatured proteins new

long range ion pairs are formed to minimize energy[65]; and (ii) protein unfolding exposes the hydrophobic protein core to the aqueous phase. This exposure of the hydrophobic core increases the availability of negatively charged groups, which are exposed to the aqueous phase.[66] In addition, the transformation from a hydrophobic to a hydrophilic environment can affect the sodium TQ signal.[67] Our current experiments cannot distinguish between the two effects referenced above, which can potentially cause the observed TQ signal to increase during a rising degree of protein denaturation. It is interesting to note that the effect (ii) correlates with the change in the slow fraction A_{SQS}/A_{SQ}. This ratio is getting close to the theoretical value of 40% for 6-8 M urea due to the change of environment from hydrophobic to hydrophilic. This process results in one or more sites with similar relaxation properties for all sodium ions. In accordance with our results, Uzman[43] observed that a larger fraction of an organic anion was bound to denatured BSA compared with native BSA.

The observed TQ signal dependence on the protein folding state could be of importance for analysis of sodium TQ signals in diseases associated with pathological changes in protein expression, such as cancer and neurodegenerative diseases. Recent studies[24,68,69] showed a reduced sodium TQ signal in cancer, whereas in recurrent cancer an increased TQ signal was demonstrated.[70] In cancer, a reduction in the sodium TQ signal could be caused by reduced extracellular pH[31] and decreased protein content in the tumor core[71] due to edema and necrosis. On the other hand, the intracellular sodium content,[72] intracellular pH[31] and the protein content in the tumor rim[71] are increased, which could lead to an increase in the sodium TQ signal. Based on our results, the increase of available negatively charged groups in misfolded proteins can also lead to an increase in sodium TQ signal. The contribution of each environmental change to the altered TQ signal in cancer has yet to be investigated to obtain a deeper understanding of the TQ signal origin in different pathologies. In addition, the influence of protein denaturation processes on the *in vivo* sodium TQ signal, where many confounding factors are present, remains to be verified. Misfolded proteins also tend to form aggregates, which could also affect the sodium TQ signal.

There is a recent debate about the possibility of discriminating between intra- and extracellular sodium signal based on the sodium TQ signal.[13,56] It was shown experimentally that the intracellular sodium signal contributes 30%-70% to the total TQ signal.[4–11] The TQ signal may have a higher intracellular sensitivity compared with the SQ signal but it cannot discriminate between extra- and intracellular signals. The TQ signal might correlate with intracellular sodium changes, as shown in an isolated well perfused rat heart system when extracellular sodium remained unchanged.[4] However, the TQ signal is influenced by many parameters, as indicated in our study, which requires a careful interpretation of TQ signal alterations before making any final conclusions about its possible correlation with intracellular sodium.

In the current study, the influence of B_0 and B_1^+ inhomogeneity on the TQ signal was minimized in order to prevent a reduction in the TQ signal.[73–75] The use of a 20-step shim routine including the first and second order shims resulted in a full width at half maximum (FWHM) of the sodium SQ signal of 25-30 Hz for all phantoms. This good B_0 homogeneity was confirmed by a minimal B_0 deviation of −90 to 240 Hz in two exemplary B_0 maps (Figure S3). Furthermore, the TQTPPI pulse sequence included a 180° RF pulse to compensate for B_0 inhomogeneity (Figure 2A). With respect to B_1^+, the use of a volume coil and the placement of all phantoms in the homogeneous part of the volume coil minimized the effect of B_1^+ inhomogeneity in our experiments. Accurate repositioning of all phantoms provided similar minimum B_1^+ deviations for all phantoms. Exemplary B_1^+ maps for both phantom sizes showed a minimal B_1^+ deviation of less than 7.2% (Figure S4). Based on calculations of Wigner matrix elements[76] and transfer functions,[77] the B_1^+ deviation of 7.2% resulted in a negligible TQ signal contribution, which was created by an imperfect refocusing pulse, of 1.8% to the total TQ signal. Any DQ signals created by an imperfect refocusing pulse were cancelled by the phase alteration of the third RF pulse.

5 | CONCLUSION

The unique capability of the TQTPPI sequence was applied to evaluate two major effects of environments on the sodium TQ signal from BSA protein solutions. The high pH values yielded up to a 225% increase of the sodium TQ signal relative to low pH. Up to a 40% increase of the sodium TQ signal was observed during protein unfolding by urea while the pH values were kept unchanged. The protein unfolding was independently controlled by fluorescence microscopy. Thus, the sodium TQ signal is closely linked to the protein structure and the availability of negatively charged groups. The results of these experiments provide a first assessment of the possible effects from pH and protein unfolding during in vivo application of the TQ signals.

ACKNOWLEDGEMENTS

The authors thank Christian Schwerk and Carolin Stump-Guthier for their support with the fluorescence measurements. V.D.S. would like to acknowledge the support from the National Science Foundation through NSF/DMR-1644779 and the state of Florida.

ORCID

Dennis Kleimaier https://orcid.org/0000-0002-7885-7675
Victor Schepkin https://orcid.org/0000-0001-5475-2636
Ruomin Hu https://orcid.org/0000-0003-3036-0691
Lothar R. Schad https://orcid.org/0000-0002-5347-9364

REFERENCES

1. Hu R, Kleimaier D, Malzacher M, Hoesl MAU, Paschke NK, Schad LR. X-nuclei imaging: Current state, technical challenges, and future directions. *J Magn Reson Imaging*. 2020;51(2):355-376.
2. Thulborn KR. Quantitative sodium MR imaging: A review of its evolving role in medicine. *Neuroimage*. 2018;168:250-268.
3. Schepkin VD, Neubauer A, Nagel AM, Budinger TF. Comparison of potassium and sodium binding in vivo and in agarose samples using TQTPPI pulse sequence. *J Magn Reson*. 2017;277:162-168.
4. Schepkin VD, Choy IO, Budinger TF, et al. Sodium TQF NMR and intracellular sodium in isolated crystalloid perfused rat heart. *Magn Reson Med*. 1998;39(4):557-563.
5. Knubovets T, Shinar H, Navon G. Quantification of the contribution of extracellular sodium to Na-23 multiple-quantum-filtered NMR spectra of suspensions of human red blood cells. *J Magn Reson*. 1998;131(1):92-96.
6. Eykyn TR, Aksentijevic D, Aughton KL, Southworth R, Fuller W, Shattock MJ. Multiple quantum filtered (23)Na NMR in the Langendorff perfused mouse heart: Ratio of triple/double quantum filtered signals correlates with [Na]i. *J Mol Cell Cardiol*. 2015;86:95-101.
7. Dizon JM, Tauskela JS, Wise D, Burkhoff D, Cannon PJ, Katz J. Evaluation of triple-quantum-filtered ^{23}Na NMR in monitoring of Intracellular Na content in the perfused rat heart: comparison of intra- and extracellular transverse relaxation and spectral amplitudes. *Magn Reson Med*. 1996;35(3):336-345.
8. Jelicks LA, Gupta RK. On the extracellular contribution to multiple quantum filtered ^{23}Na NMR of perfused rat heart. *Magn Reson Med*. 1993;29(1):130-133.
9. Seshan V, Sherry AD, Bansal N. Evaluation of triple quantum-filtered ^{23}Na NMR spectroscopy in the in situ rat liver. *Magn Reson Med*. 1997;38(5):821-827.
10. Winter PM, Bansal N. Triple-quantum-filtered ^{23}Na NMR spectroscopy of subcutaneously implanted 9l gliosarcoma in the rat in the presence of TmDOTP(5-1). *J Magn Reson*. 2001;152(1):70-78.
11. Schepkin VD, Choy IO, Budinger TF. Sodium alterations in isolated rat heart during cardioplegic arrest. *J Appl Physiol*. 1996;81(6):2696-2702.
12. Neubauer A, Nies C, Schepkin VD, et al. Tracking protein function with sodium multi quantum spectroscopy in a 3D-tissue culture based on microcavity arrays. *Sci Rep*. 2017;7(1):3943.
13. Hoesl MAU, Kleimaier D, Hu R, et al. ^{23}Na Triple-quantum signal of in vitro human liver cells, liposomes, and nanoparticles: Cell viability assessment vs. separation of intra- and extracellular signal. *J Magn Reson Imaging*. 2019;50(2):435-444.
14. Choy IO, Schepkin VD, Budinger TF, Obayashi DY, Young JN, DeCampli WM. Effects of specific sodium/hydrogen exchange inhibitor during cardioplegic arrest. *Ann Thorac Surg*. 1997;64(1):94-99.
15. Schepkin VD, Choy IO, Budinger TF, Young JN, DeCampli WM. Multi-dose crystalloid cardioplegia preserves intracellular sodium homeostasis in myocardium. *J Mol Cell Cardiol*. 1999;31(9):1643-1651.
16. LaVerde G, Nemoto E, Jungreis CA, Tanase C, Boada FE. Serial triple quantum sodium MRI during non-human primate focal brain ischemia. *Magn Reson Med*. 2007;57(1):201-205.
17. Neumaier-Probst E, Konstandin S, Ssozi J, et al. A double-tuned ^{1}H/^{23}Na resonator allows ^{1}H-guided ^{23}Na-MRI in ischemic stroke patients in one session. *Int J Stroke*. 2015;10((Suppl A100)):56-61.
18. Ouwerkerk R, Bleich KB, Gillen JS, Pomper MG, Bottomley PA. Tissue sodium concentration in human brain tumors as measured with ^{23}Na MR imaging. *Radiology*. 2003;227(2):529-537.
19. Schepkin VD, Chenevert TL, Kuszpit K, et al. Sodium and proton diffusion MRI as biomarkers for early therapeutic response in subcutaneous tumors. *Magn Reson Imaging*. 2006;24(3):273-278.
20. Schepkin VD, Lee KC, Kuszpit K, et al. Proton and sodium MRI assessment of emerging tumor chemotherapeutic resistance. *NMR Biomed*. 2006;19(8):1035-1042.
21. Schepkin VD, Ross BD, Chenevert TL, et al. Sodium magnetic resonance imaging of chemotherapeutic response in a rat glioma. *Magn Reson Med*. 2005;53(1):85-92.
22. Zaric O, Pinker K, Zbyn S, et al. Quantitative sodium MR imaging at 7 T: initial results and comparison with diffusion-weighted imaging in patients with breast tumors. *Radiology*. 2016;280(1):39-48.
23. Rooney WD, Li X, Sammi MK, Bourdette DN, Neuwelt EA, Springer CS Jr. Mapping human brain capillary water lifetime: high-resolution metabolic neuroimaging. *NMR Biomed*. 2015;28(6):607-623.
24. Fiege DP, Romanzetti S, Mirkes CC, Brenner D, Shah NJ. Simultaneous single-quantum and triple-quantum-filtered MRI of ^{23}Na (SISTINA). *Magn Reson Med*. 2013;69(6):1691-1696.
25. Worthoff WA, Shymanskaya A, Shah NJ. Relaxometry and quantification in simultaneously acquired single and triple quantum filtered sodium MRI. *Magn Reson Med*. 2019;81(1):303-315.
26. Hoesl MAU, Schad LR, Rapacchi S. Efficient ^{23}Na triple-quantum signal imaging on clinical scanners: Cartesian imaging of single and triple-quantum ^{23}Na (CRISTINA). *Magn Reson Med*. 2020.
27. Jelicks LA, Gupta RK. Double-quantum NMR of sodium ions in cells and tissues - paramagnetic quenching of extracellular coherence. *J Magn Reson*. 1989;81(3):586-592.
28. van der Maarel JRC. Thermal relaxation and coherence dynamics of spin 3/2. II. Strong radio-frequency field. *Concepts Magn Reson*. 2003;19A(2):117-133.
29. van der Maarel JRC. Relaxation of spin quantum number S=3/2 under multiple-pulse quadrupolar echoes. *J Chem Phys*. 1991;94(7):4765-4775.
30. Fonseca CP, Fonseca LL, Montezinho LP, et al. ^{23}Na multiple quantum filtered NMR characterisation of Na^+ binding and dynamics in animal cells: a comparative study and effect of Na^+/Li^+ competition. *Eur Biophys J*. 2013;42(7):503-519.
31. White KA, Grillo-Hill BK, Barber DL. Cancer cell behaviors mediated by dysregulated pH dynamics at a glance. *J Cell Sci*. 2017;130(4):663-669.
32. Kobatake K, Sako K, Izawa M, Yamamoto YL, Hakim AM. Autoradiographic determination of brain pH following middle cerebral artery occlusion in the rat. *Stroke*. 1984;15(3):540-547.
33. Nedergaard M, Kraig RP, Tanabe J, Pulsinelli WA. Dynamics of interstitial and intracellular pH in evolving brain infarct. *Am J Physiol*. 1991;260(3 Pt 2):R581-R588.

34. Sako K, Kobatake K, Yamamoto YL, Diksic M. Correlation of local cerebral blood flow, glucose utilization, and tissue pH following a middle cerebral artery occlusion in the rat. *Stroke*. 1985;16(5):828-834.
35. Kumar S, Nussinov R. Close-range electrostatic interactions in proteins. *Chembiochem*. 2002;3(7):604–617.
36. Carr CW. Studies on the binding of small ions in protein solutions with the use of membrane electrodes. VI. The binding of sodium and potassium ions in solutions of various proteins. *Arch Biochem Biophys*. 1956;62(2):476-484.
37. Pfister H, Pauly H. Membranpotential und Ionenbindung in Proteinlsungen. *Biophysik*. 1964;1(4):364-369.
38. Saroff HA. The binding of ions to the muscle proteins. A theory for K+ and Na+ binding based on a hydrogen-bonded and chelated model. *Arch Biochem Biophys*. 1957;71(1):194-203.
39. Hutchison RB, Malhotra D, Hendrick RE, Chan L, Shapiro JI. Evaluation of the double-quantum filter for the measurement of intracellular sodium concentration. *J Biol Chem*. 1990;265(26):15506-15510.
40. Das A, Mukhopadhyay C. Urea-mediated protein denaturation: a consensus view. *J Phys Chem B*. 2009;113(38):12816-12824.
41. Matouschek A, Kellis JT Jr, Serrano L, Fersht AR. Mapping the transition state and pathway of protein folding by protein engineering. *Nature*. 1989;340(6229):122-126.
42. Heinrich PC, Müller M, Graeve L. *Löffler/Petrides Biochemie und Pathobiochemie*. Berlin Heidelberg: Springer; 2014.
43. Uzman LL. Organic anion binding by denatured bovine serum albumin. *Nature*. 1953;171(4354):653-654.
44. Schepkin VD. Statistical tensor analysis of the MQ MR signals generated by weak quadrupole interactions. *Z Med Phys*. 2019;29(4):326-336.
45. Torres AM, Philp DJ, Kemp-Harper R, Garvey C, Kuchel PW. Determination of Na^+ binding parameters by relaxation analysis of selected ^{23}Na NMR coherences: RNA, BSA and SDS. *Magn Reson Chem*. 2005;43(3):217-224.
46. Rooney WD, Springer CS. The molecular environment of intracellular sodium: ^{23}Na NMR relaxation. *NMR Biomed*. 1991;4(5):227-245.
47. Chung C-W, Wimperis S. Optimum detection of biexponential relaxation using multiple-quantum filtration techniques. *J Magn Reson*. 1990;88(2):440-447.
48. Zaiss M, Kunz P, Goerke S, Radbruch A, Bachert P. MR imaging of protein folding in vitro employing nuclear-Overhauser-mediated saturation transfer. *NMR Biomed*. 2013;26(12):1815-1822.
49. Pace CN. Determination and analysis of urea and guanidine hydrochloride denaturation curves. *Methods Enzymol*. 1986;131:266-280.
50. Grimsley GR, Scholtz JM, Pace CN. A summary of the measured pK values of the ionizable groups in folded proteins. *Protein Sci*. 2009;18(1):247-251.
51. Katsuta K, Hatakeyama M, Hiraki J. Isothermal gelation of proteins. 1. Urea-induced gelation of whey proteins and their gelling mechanism. *Food Hydrocoll*. 1997;11(4):367-372.
52. Moré JJ, Sorensen DC. Computing a Trust Region Step. *SIAM J Sci Statist Comput*. 1983;4(3):553-572.
53. Wenzel TJ, Skoog DA, West DM, Holler JF, Crouch SR. *Fundamentals of Analytical Chemistry*. Boston, MA: Cengage Learning; 2013.
54. Knubovets T, Shinar H, Eliav U, Navon G. A 23Na multiple-quantum-filtered NMR study of the effect of the cytoskeleton conformation on the anisotropic motion of sodium ions in red blood cells. *J Magn Reson B*. 1996;110(1):16-25.
55. Lin VJ, Koenig JL. Raman studies of bovine serum albumin. *Biopolymers*. 1976;15(1):203-218.
56. Burstein D, Springer CS Jr. Sodium MRI revisited. *Magn Reson Med*. 2019;82(2):521-524.
57. Marathe K, McVicar N, Li A, Bellyou M, Meakin S, Bartha R. Topiramate induces acute intracellular acidification in glioblastoma. *J Neurooncol*. 2016;130(3):465-472.
58. Makela HI, Grohn OH, Kettunen MI, Kauppinen RA. Proton exchange as a relaxation mechanism for T1 in the rotating frame in native and immobilized protein solutions. *Biochem Biophys Res Commun*. 2001;289(4):813-818.
59. Moon RB, Richards JH. Determination of intracellular pH by ^{31}P Magnetic Resonance. *J Biol Chem*. 1973;248(20):7276-7278.
60. Pavuluri K, McMahon MT. pH imaging using Chemical Exchange Saturation Transfer (CEST) MRI. *Isr J Chem*. 2017;57(9):862-879.
61. Kalyanapuram R, Seshan V, Bansal N. Three-dimensional triple-quantum-filtered ^{23}Na imaging of the dog head in vivo. *J Magn Reson Imaging*. 1998;8(5):1182-1189.
62. Tauskela JS, Dizon JM, Whang J, Katz J. Evaluation of multiple-quantum-filtered ^{23}Na NMR in monitoring intracellular Na content in the isolated perfused rat heart in the absence of a chemical-shift reagent. *J Magn Reson*. 1997;127(1):115-127.
63. Colet JM, Bansal N, Malloy CR, Sherry AD. Multiple quantum filtered ^{23}Na NMR spectroscopy of the isolated, perfused rat liver. *Magn Reson Med*. 1999;41(6):1127-1135.
64. Bansal N, Seshan V. Three-dimensional triple quantum-filtered ^{23}Na imaging of rabbit kidney with weighted signal averaging. *J Magn Reson Imaging*. 1995;5(6):761-767.
65. Pace CN, Shaw KL. Linear extrapolation method of analyzing solvent denaturation curves. *Proteins*. 2000;41(S4):1-7.
66. Ui N. Conformational studies on proteins by isoelectric focusing. *Ann N Y Acad Sci*. 1973;209:198-209.
67. Rooney WD, Springer CS Jr. A comprehensive approach to the analysis and interpretation of the resonances of spins 3/2 from living systems. *NMR Biomed*. 1991;4(5):209-226.
68. Schepkin VD, Gawlick U, Ross BD, Chenevert TL. Detection of triple quantum Na NMR in normal and tumored mouse brain. *Proc Int Soc Magn Reson Med*. 2003;11:39.
69. Choi CH, Stegmayr C, Shymanskaya A, et al. Feasibility study of multinuclear MR at 9.4T and PET in a rat brain tumor model. *Proc Int Soc Magn Reson Med*. 2018;26:3032.
70. Boada FE, Davis D, Walter K, et al. Triple quantum filtered sodium MRI of primary brain tumors. 2004 2nd IEEE International Symposium on Biomedical Imaging: Nano to Macro (IEEE Cat No. 04EX821), Arlington, VA, USA. 2004;2:1215–1218. https://doi.org/10.1109/ISBI.2004.1398763
71. Ray KJ, Simard MA, Larkin JR, et al. Tumor pH and protein concentration contribute to the signal of amide proton transfer magnetic resonance imaging. *Cancer Res*. 2019;79(7):1343-1352.
72. Cameron IL, Smith NK, Pool TB, Sparks RL. Intracellular concentration of sodium and other elements as related to mitogenesis and oncogenesis in vivo. *Cancer Res*. 1980;40(5):1493-1500.
73. Hancu I, Boada FE, Shen GX. Three-dimensional triple-quantum-filtered ^{23}Na imaging of in vivo human brain. *Magn Reson Med*. 1999;42(6):1146-1154.
74. Matthies C, Nagel AM, Schad LR, Bachert P. Reduction of B(0) inhomogeneity effects in triple-quantum-filtered sodium imaging. *J Magn Reson*. 2010;202(2):239-244.

75. Tanase C, Boada FE. Triple-quantum-filtered imaging of sodium in presence of B(0) inhomogeneities. *J Magn Reson*. 2005;174(2):270-278.
76. Müller N, Bodenhausen G, Ernst RR. Relaxation-induced violations of coherence transfer selection rules in nuclear magnetic resonance. *J Magn Reson*. 1987;75(2):297-334.
77. van der Maarel JRC. Thermal relaxation and coherence dynamics of spin 3/2. I. Static and fluctuating quadrupolar interactions in the multipole basis. *Concepts Magn Reson*. 2003;19A(2):97-116.

SUPPORTING INFORMATION

Additional supporting information may be found online in the Supporting Information section at the end of this article.

How to cite this article: Kleimaier D, Schepkin V, Hu R, Schad LR. Protein conformational changes affect the sodium triple-quantum MR signal. *NMR in Biomedicine*. 2020;e4367. https://doi.org/10.1002/nbm.4367